

2.7 OBSERVATIONS OF EKMAN SPIRALS AND EKMAN TRANSPORT NEAR THE KERGUELEN PLATEAU

Christopher J. Roach*

Institute for Marine and Antarctic Studies, University of Tasmania, Hobart, Tasmania

Helen E. Phillips

Institute for Marine and Antarctic Studies, University of Tasmania, Hobart, Tasmania

Nathaniel L. Bindoff

CSIRO Marine and Atmospheric Research; ACECRC; CAWRC and Institute for Marine and Antarctic Studies,
University of Tasmania, Hobart, Tasmania

Steve R. Rintoul

CSIRO Marine and Atmospheric Research; ACECRC and CAWRC, Hobart, Tasmania

1. Introduction

V.W. Ekman's theory of wind forcing on the ocean is a corner stone of oceanography. By considering a balance between frictional and Coriolis forces and assuming a constant vertical eddy viscosity, Ekman (1905) devised equations for the latitudinal and longitudinal velocity components as a function of depth. For steady winds the resulting solution is the Ekman spiral which has a characteristic exponential velocity amplitude decay and anticyclonic (anticlockwise in the Southern Hemisphere) rotation with increasing depth. The net transport arising from Ekman currents is of significance in meridional overturning circulation, driving the upwelling of deep waters (Speer et al. 2000) and transporting them northward. It may also be significant in the formation of Mode Waters (Sallée et al. 2006).

Previous studies have established the validity of the relationship between wind stress and net Ekman transport and observed Ekman-like spirals in data averaged over long time periods in a coordinate frame relative to the wind. However, details of the vertical structure of net transport are still not fully resolved and the detection of Ekman

spirals over short time frames remains rare.

Additionally, within the Southern Ocean Ekman transport and Ekman currents have been the subject of few previous studies (Elipot 2006; Lenn and Chereskin 2009). This study makes use of velocity data from eight EM-APEX floats to investigate these issues.

2. The Dataset

EM-APEX floats are a development of the APEX sub-surface profiling float which makes up much of the current Argo fleet. EM-APEX floats (Sanford et al. 2005) are equipped with a set of rotation vanes and five electrodes, four of which are arranged to form two orthogonal and independent voltage-measuring axes. Voltage measurements taken between these electrodes can be converted to velocities relative to the depth-integrated horizontal velocity (Sanford et al. 1978). This depth independent offset can be estimated from the displacement between the float's descent and surfacing locations allowing absolute velocities to be calculated. EM-APEX floats are equipped to use the IRIDIUM satellite system, allowing two-way communication.

The data used in this study was collected using eight EM-APEX floats deployed north of Kerguelen Island in November 2008 in conjunction with the SOFINE expedition (Figure 1). The floats

*Corresponding author address: Christopher J. Roach, Univ. of Tasmania, Institute for Marine and Antarctic Studies, Hobart, Tasmania, Australia; email croach@utas.edu.au

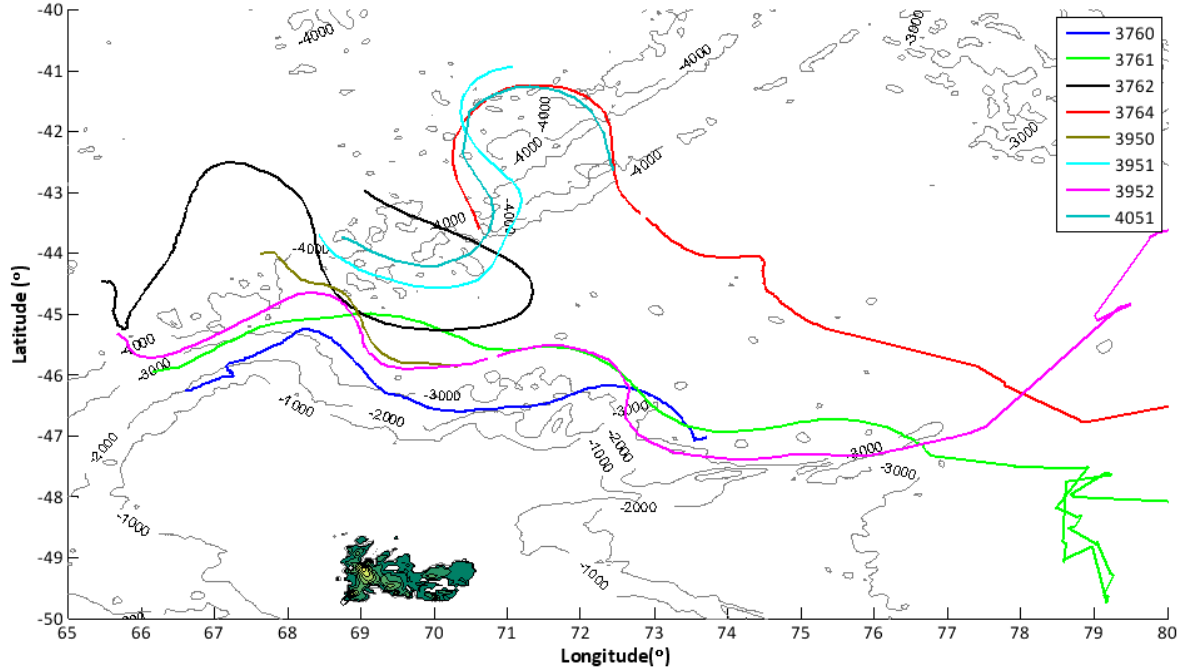


Figure 1: Trajectories of the eight EM-APEX floats employed in this study.

returned over 1600 profiles with vertical resolution of between 3 and 6m. While within the Kerguelen Island region all floats took four profiles (two descent-ascent cycles) per day. Once downstream of Kerguelen Island surviving floats were reprogrammed to follow the standard Argo cycle of approximately 10 days between profiles.

3. Method

a. Isolating Ekman Currents

In order to isolate Ekman velocities from the absolute velocity profiles generated by the EM-APEX floats both geostrophic currents and inertial oscillations had to be removed. During this study the latitude of the EM-APEX floats ranged from 41°S to 49°S, with inertial periods between 15.9 and 18.2 hours. The profiling mission was designed to ensure that while near Kerguelen Island the pairs of adjacent up casts or down casts were separated by approximately half an inertial period.

The complex velocity between each half-inertial pair of casts was modelled as the sum of a steady subinertial complex velocity Z_M and a time varying complex near-inertial velocity Z_I (Phillips 2010). The inertial velocity was described by the equation:

$$Z_I = A_I \times e^{i(\phi - ft)} \quad (1)$$

Where A_I denotes the amplitude of the inertial current, ϕ denotes the phase and f denotes the coriolis parameter.

Values of A_I and ϕ were estimated from observations and the resulting Z_I was subtracted to isolate the subinertial velocity between each half-inertial pair.

Having filtered near-inertial frequencies out of the velocity profiles it was necessary to remove the geostrophic component to isolate the Ekman currents. Calculation of geostrophic velocities from the hydrographic data collected by the floats was ruled out as it would only provide the cross-track component of velocity. Hence, the only feasible option was to assume that the geostrophic component could be approximated by a reference velocity taken at such a depth that the Ekman component has decayed to an insignificant level. This method has been applied with a degree of success during a number of previous studies (Chereskin 1995; Lenn and Chereskin 2009). Previous studies have observed behaviour potentially indicative of coupling between Ekman decay scales and mixed layer depth (Price et al. 1987), thus it is necessary to select a reference

depth below the typical mixed layer depth. Within the Kerguelen region a prior observations (Sallée et al. 2006) indicated mixed layer depths (MLDs) of less than 100m in summer and up to 200m in winter. On this basis the reference velocity to be used as a proxy for the geostrophic velocity for each profile was defined as the mean velocity between 200m and 300m.

b. Estimating Ekman Decay Scales and Eddy Viscosities

Examination of solutions of Ekman's equations for the Southern Hemisphere indicates that a complex Ekman velocity can be separated into a speed component decaying exponentially with increasing depth and a unit vector component rotating anticlockwise as a linear function of increasing depth:

$$|u_{ek} + iv_{ek}| = V_{surf} e^{\frac{z}{D_e}} \quad (2a)$$

$$\theta(z) = \frac{z}{D_e} \quad (2b)$$

Where D_e is the e-folding depth and $\theta(z)$ is the heading of the Ekman velocity relative to the surface Ekman velocity at depth z (positive upwards), with rotation clockwise taken to be positive with increasing depth. Negative values of D_e obtained from equation 2b correspond to clockwise rotation with increasing depth while positive values correspond to anticlockwise rotation with depth.

Equations 2a and 2b were fitted to the upper 50m of the velocity profiles using a least squares technique, providing estimates of D_e . The fraction of variance (R^2 value) within the data captured by equations 2a and 2b was calculated for each profile. If the amplitude R^2 exceeded 0.75; the rotational R^2 exceeded 0.5 and a 'logical' e-folding depth (less than 1000m) was obtained, the profile was classified as displaying a spiral and the

direction of rotation was obtained from the sign of the rotational e-folding depth.

Additionally, in line with other prior studies (Schudlich and Price 1998) all profiles were rotated into a wind-relative reference frame using wind estimates obtained from the NCEP surface wind fields before a mean wind-relative profile was calculated.

c. Calculating Cross-wind and Cross-track Transports

To examine the vertical structure of Ekman transport, previous studies (Chereskin and Roemmich 1991; Wijffels et al. 1994) undertaken in bands of westerly winds in the tropics have used ship-mounted ADCPs and hydrographic transects to isolate the cross-ship-track component of the Ekman velocities. Here, we attempt to apply a similar approach along the tracks of each of the eight EM-APEX floats.

Due to the more complex nature of the float trajectories and the more variable winds in the Kerguelen island region, Ekman transport was examined in a cross-wind reference frame rather than the cross-track reference frame used in previous studies. Cross-wind Ekman velocities were obtained by taking Ekman velocities isolated using the technique described in section 3a before rotating each profile into a wind based reference frame. All Ekman velocity profiles were mapped onto a regular 2m depth grid. Transport between each depth level and the 200m level was then calculated using trapezoidal numerical integration.

Potential density profiles were calculated and mixed layer depth identified using a density criteria of $\Delta\sigma > 0.03 \text{ kg m}^{-3}$ relative to the upper most observation (Sallée et al. 2006) before each vertically integrated transport profile was interpolated onto a regular fraction-of-MLD axis. Transport between the fraction-MLD levels was determined by taking the difference of vertically integrated transport between adjacent MLD levels.

Mean profiles of cross-wind transport per unit path length were calculated while net transport

profiles were computed by integrating the transport within each fraction-of-MLD layer along the float track.

($308\text{-}2210\text{cm}^2\text{s}^{-1}$) obtained by a previous study in the Drake Passage (Lenn and Chereskin 2009). The ratio of amplitude and rotational e-folding depths was calculated for all Ekman spiral and a

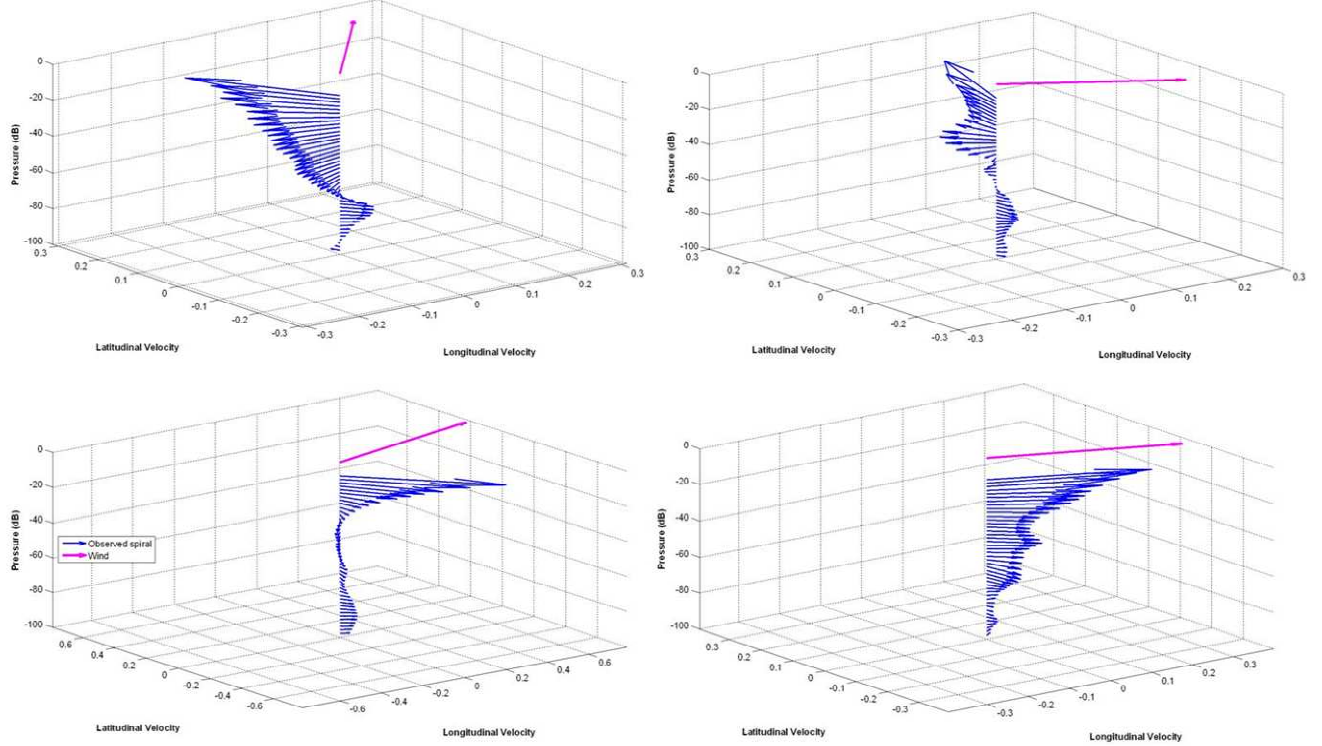


Figure 2: Example Ekman-like spirals (top left: Float 3760 cast 22, top right: Float 3764 cast 132) and reversed spirals (bottom left: Float 3760 cast 11, bottom right: Float 3952 cast 158).

4. Observed Ekman Spirals

A total of 285 spirals displaying anticlockwise rotation and exponentially decaying current speed were detected and judged to be qualitatively consistent with steady state Ekman solutions. Furthermore 215 spirals with Ekman-like decay and reverse rotation, possibly consistent with cyclonic super-inertial wind forcing (Rudnick and Weller 1993), were detected. Examples of both anticlockwise and clockwise spirals are shown in Figure 2.

Estimates of e-folding depth from velocity amplitude decay were found to be inconsistent with estimates from current rotation with depth. The mean e-folding depth obtained from the amplitude fits was 25m with a corresponding eddy viscosity of $580\text{cm}^2\text{s}^{-1}$, while the mean over the rotational fits gave values of 40m and $1500\text{cm}^2\text{s}^{-1}$ respectively. These values are within the range of estimates

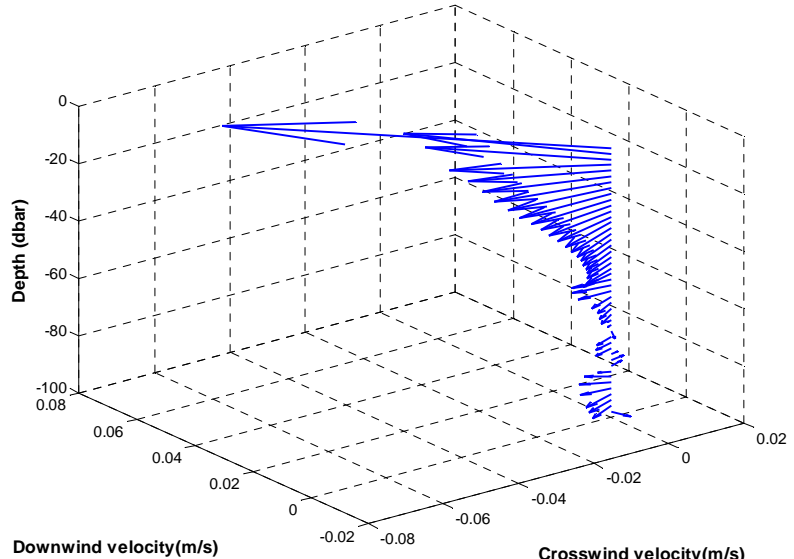


Figure 2: The wind relative mean spiral.

mean value computed, giving a ratio of 1:1.95. This is consistent with previous observational studies (Chereskin 1995; Lenn and Chereskin 2009; Price et al. 1987) that found Ekman spirals displaying a

similar 1:2 ratio. This ‘compression’ of the spiral was also observed in the wind-relative mean profile (Figure 3).

It is clear that the e-folding depths we have observed are not consistent with classical steady state Ekman theory. Hence, additional factors such as stratification, variation of eddy viscosity with depth or temporal variation in the wind forcing must be considered.

5. Vertical Structure of Ekman Transport

Profiles of crosswind transport integrated along floats tracks are shown in Figure 4, negative values denote transport to the left of the wind. Mean mixed layer depth for individual floats ranges from 29m to 51m. The majority of profiles display intensification of crosswind transport for shallow depths.

Five of the eight integrated crosswind

than 0.5MLD have been neglected as much of this range impinges onto the 0-15m range in which little velocity data was recorded, hence distorting transport estimates. Of the three remaining floats: one (Float 3760) displays well defined decay between 0.5MLD and 1MLD but suffers from noisy data at deeper levels; Float 3951 displays no significant trend and Float 3764 displays slab-like behaviour with transport to the right of the wind between 0.5 and 1MLD. The same general patterns were also observed in the corresponding mean transport profiles (not shown).

The fact that in the majority of both along-track integrated transport and mean transport profiles transport is largely confined to the mixed layer is suggestive of some form of coupling between stratification and momentum mixing. This is consistent with a number of prior observations

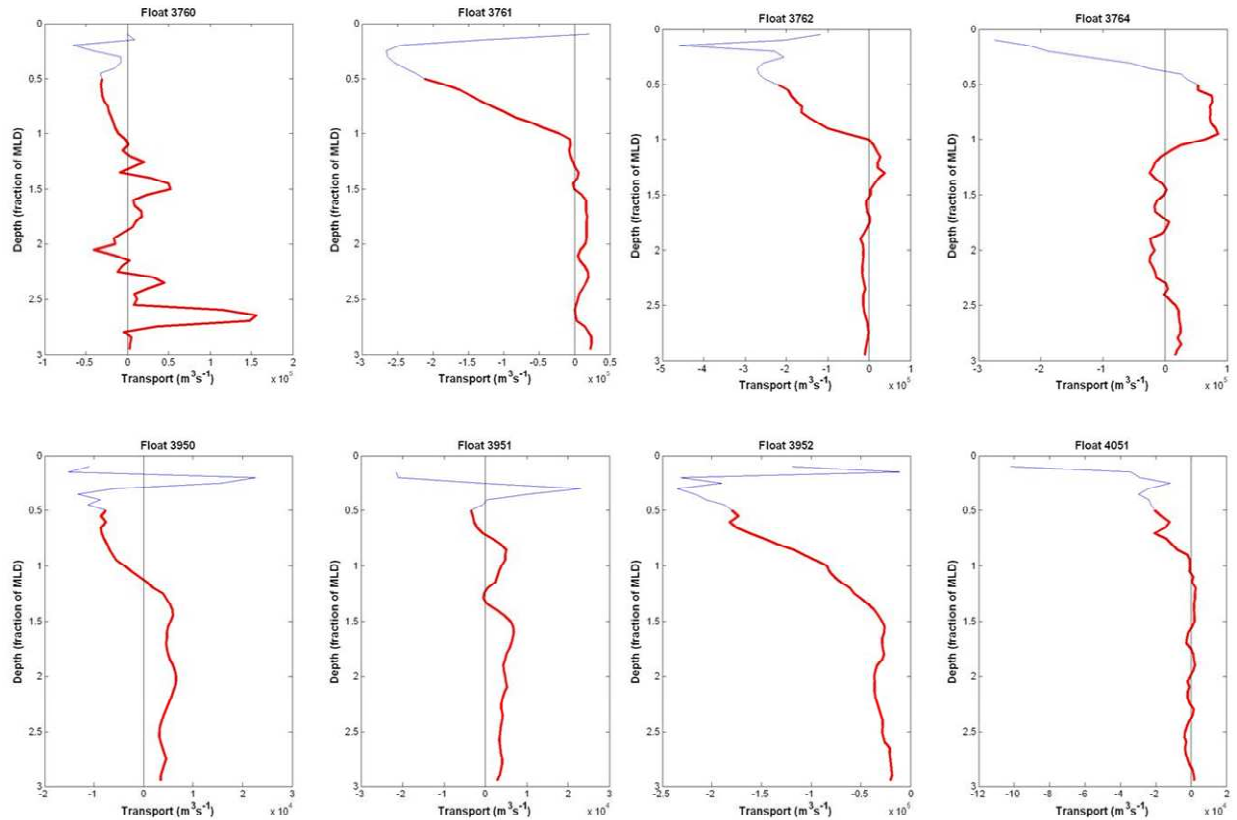


Figure 3: Profiles of crosswind transport integrated along float trajectories for all EM-APEX floats. The blue line marks sections of each profile at less than 0.5 mixed layer depths which typically coincides with ranges of ‘real’ depths for which velocity measurements were sparse.

transport profiles display transport to the left of the wind above 1MLD; a well defined decay in transport amplitude between 0.5MLD and 1MLD and near constant transport below 1MLD. Depths shallower

and modified versions of Ekman theory (Price and Sundermeyer 1999; Price et al. 1987). The decay in transport amplitudes observed in the integrated and mean transport profiles is indicative that in contrast

to the findings of studies undertaken in the North Pacific (McNally and White 1985; Wijffels et al. 1994), a slab-like model (constant transport and Ekman velocity within the mixed layer) is not an appropriate representation of Ekman transport in the vicinity of the Antarctic Circumpolar Current.

6. Conclusion

We have successfully isolated near surface ageostrophic velocities from data collected using EM-APEX velocity profiling floats. This data has been analysed and 285 profiles displaying Ekman-like spirals were identified. By applying least square fits to the speed and rotation of each spiral estimates of e-folding depth and eddy viscosity were made. Estimates of e-folding depth from velocity amplitude decay were found to be inconsistent with estimates from current heading. Typically, spirals were found to be ‘compressed’: the rotational e-folding depth being approximately twice the amplitude of decay e-folding depth. This is consistent with a number of previous studies (Lenn and Chereskin, 2009, Price and Sundermeyer, 1999, Price et al., 1987). This result is reflected in the mean eddy viscosities of $580\text{cm}^2\text{s}^{-1}$ and $1500\text{cm}^2\text{s}^{-1}$ obtained from the rotational and amplitude fits respectively. These values are consistent with results from the Drake Passage (Lenn and Chereskin, 2009). Overall, these observations are not consistent with ‘classical’ steady state Ekman theory in which a constant eddy viscosity is assumed.

Examination of crosswind transport integrated along float trajectories indicates that, generally, at depths greater than approximately 1.5 mixed layer depths transport is constant. At depths shallower than 1 to 1.5 MLDs transport was more intense and usually intensified approaching the surface, a behaviour which is not consistent with a slab-like model. In the majority of trajectory-integrated crosswind transport is to the left of the wind, consistent with Ekman theory. This consistent onset of intensification at 1 to 1.5 MLD suggests that there is some form of coupling between the

penetration of Ekman transport and mixed layer depth.

Further examination of several features noted in this study will be necessary. The 215 profiles displaying reversed spirals must be investigated to establish any links with cyclonic super-inertial wind forcing (Rudnick and Weller 1993), this will be approached by applying rotary spectral analysis to ship-board wind observations taken during the voyage on which the EMAPEX float were deployed. Further investigation is also required to confirm the apparent coupling between cross-wind Ekman transport and the stratification associated with mixed layer depth.

Bibliography:

- Chereskin, T. K., 1995: Direct evidence for an Ekman balance in the California Current. *Journal Of Geophysical Research*, 100, 18261-18269.
- Chereskin, T. K., and D. Roemmich, 1991: A Comparison of Measured and Wind-derived Ekman Transport at 11°N in the Atlantic Ocean. *Journal Of Physical Oceanography*, 21, 869-878.
- Ekman, V. W., 1905: On the Influence of the Earth's Rotation on Ocean Currents. *Ark. Mat. Astron. Fys.*, 2, 1-52.
- Elipot, S., 2006: Spectral characterization of Ekman velocities in the Southern Ocean based on surface drifter trajectories, Scripps Institution of Oceanography, University of California.
- Lenn, Y., and T. K. Chereskin, 2009: Observation of Ekman Currents in the Southern Ocean. *Journal Of Physical Oceanography*, 39, 768-779.
- McNally, G. J., and W. B. White, 1985: Wind Driven Flow in the Mixed Layer Observed by Drifting Bouys during Autumn-Winter in the Midlatitude North Pacific. *Journal Of Physical Oceanography*, 15, 684-694.
- Phillips, H. E., 2010: Ocean Mixing In The ACC. *4th CAWCR Modelling Workshop*, A. J. Hollis, and K. A. Day, Eds., 85-88.

- Price, J. F., and M. A. Sundermeyer, 1999: Stratified Ekman Layers. *Journal Of Geophysical Research*, 104, 20467-20494.
- Price, J. F., R. A. Weller, and R. R. Schudlich, 1987: Wind-Driven Ocean Currents and Ekman Transport. *Science*, 238, 1534-1538.
- Rudnick, D. L., and R. A. Weller, 1993: Observations of Superinertial and Near-Inertial Wind-driven Flow. *Journal Of Physical Oceanography*, 23, 2351-2359.
- Sallée, J.-B., N. Wienders, K. Speer, and R. Morrow, 2006: Formation of subantarctic mode water in the southeastern Indian Ocean. *Ocean Dynamics*, 56, 525-542.
- Sanford, T. B., R. G. Drever, and J. H. Dunlap, 1978: A velocity profiler based on the principles of geomagnetic induction. *Deep-Sea Research*, 25, 183-210.
- Sanford, T. B., J. H. Dunlap, J. A. Carlson, D. C. Webb, and J. B. Girton, 2005: Autonomous velocity and density profiler: EM-APEX. *IEEE/OES Eighth Working Conference on Current Measurement Technology*, IEEE, 152-156.
- Schudlich, R. R., and J. F. Price, 1998: Observations of Seasonal Variation in the Ekman Layer. *Journal Of Physical Oceanography*, 28, 1187-1204.
- Speer, K., S. R. Rintoul, and B. Sloyan, 2000: The Diabatic Deacon Cell. *Journal Of Physical Oceanography*, 30, 3212-3222.
- Wijffels, S., E. Firing, and H. Bryden, 1994: Direct Observation of the Ekman Balance at 10°N in the Pacific. *Journal Of Physical Oceanography*, 24, 1666-1679.